How to cite: *Angew. Chem. Int. Ed.* **2020**, *59*, 22223 – 22229
International Edition: doi.org/10.1002/anie.202010199
German Edition: doi.org/10.1002/ange.202010199

Systems Chemistry

Nucleotide-Selective Templated Self-Assembly of Nanoreactors under Dissipative Conditions

*Sushmitha Chandrabhas[+], Subhabrata Maiti[+], Ilaria Fortunati, Camilla Ferrante, Luca Gabrielli, and Leonard J. Prins**

Abstract: *Nature adopts complex chemical networks to finely tune biochemical processes. Indeed, small biomolecules play a key role in regulating the flux of metabolic pathways. Chemistry, which was traditionally focused on reactions in simple mixtures, is dedicating increasing attention to the network reactivity of highly complex synthetic systems, able to display new kinetic phenomena. Herein, we show that the addition of monophosphate nucleosides to a mixture of amphiphiles and reagents leads to the selective templated formation of self-assembled structures, which can accelerate a reaction between two hydrophobic reactants. The correct matching between nucleotide and the amphiphile head group is fundamental for the selective formation of the assemblies and for the consequent up-regulation of the chemical reaction. Transient stability of the nanoreactors is obtained under dissipative conditions, driven by enzymatic dephosphorylation of the templating nucleotides. These results show that small molecules can play a key role in modulating network reactivity, by selectively templating self-assembled structures that are able to up-regulate chemical reaction pathways.*

Introduction

Complex chemical networks are used by nature to precisely regulate biochemical processes.[1,2] A key aspect is the up- or downregulation of regulatory pathways by small (bio)molecules.[3] Whereas chemistry traditionally has been dedicated to study reactions in mixtures containing just the reactants and other essential additives (e.g. catalysts), there is a growing interest in network reactivity, that is, chemical reactivity expressed by synthetic mixtures of higher complexity.[4–7] Synthetic systems relying on reaction networks are able to display new kinetic phenomena, such as oscillations, bistability, etc. that cannot be observed in traditional reaction mixtures.[8] New properties are envisioned for materials, diagnostics and delivery systems able to display such kinetics.[9–11] The general approach to constructing chemical reaction networks involves the use of mixtures of DNA,[12] peptides,[13] enzymes[14] or entirely synthetic molecules[15] in which molecular recognition between the components directly affects the kinetic evolution of the system through allosteric effects and feedback mechanisms. Yet, in this context one element has received relatively less attention, which is the role of structure formation by the mixture of components in directing kinetic evolution of the system.[16–22] From this perspective, it is important to note that recently various examples of chemically fuelled transient formation of self-assembled structures have been reported.[23–38] These examples exploit the concomitant occurrence of a fast forward reaction which activates the building blocks for self-assembly and a second, slower, deactivation reaction which leads to spontaneous disassembly. The fact that the process is chemically activated enables the exploitation of transiently formed structures in chemical reaction networks. Here, we demonstrate that the addition of monophosphate nucleosides to a mixture of amphiphiles and reactants results in the selective templated self-assembly of nanoreactors which can accelerate a bimolecular reaction between two reactants. Under dissipative conditions, installed by the presence of a dephosphorylation enzyme, a transient up-regulation of the reaction is observed. A key point of the findings presented here is that transient formation of the nanoreactors and up-regulation occur only in case of matching recognition motifs between the nucleotide and the building blocks. These results demonstrate that small molecules can play an important, indirect regulatory role in network reactivity by selectively templating structures which are able to up-regulate chemical reaction pathways (Figure 1).

Results and Discussion

We previously showed that ATP can stabilize vesicular assemblies composed of amphiphile C_{16}TACN·Zn^{2+} (TACN = 1,4,7-triazacyclononane) in aqueous buffered solution.[39,40] The presence of ATP caused a 10-fold decrease in the critical aggregation concentration (CAC) from around 100 μM to 10 μM, which implies that ATP templates assembly formation at concentrations at which the amphiphilic molecules by themselves are not assembled. In a follow-up study, we have shown that the same stabilizing effect is also exerted by other anionic molecules having multiple negatively charged groups.[41] Although these latter results affirm that templated

[*] S. Chandrabhas,[+] Dr. I. Fortunati, Prof. Dr. C. Ferrante, Dr. L. Gabrielli, Prof. Dr. L. J. Prins
Department of Chemical Sciences, University of Padova
Via Marzolo 1, 35131 Padova (Italy)
E-mail: leonard.prins@unipd.it
Dr. S. Maiti[+]
Department of Chemical Sciences, Indian Institute of Science Education and Research (IISER)
Mohali Knowledge City, Manauli 140306 (India)
[+] These authors contributed equally to this work.
Supporting information and the ORCID identification number(s) for the author(s) of this article can be found under: https://doi.org/10.1002/anie.202010199.

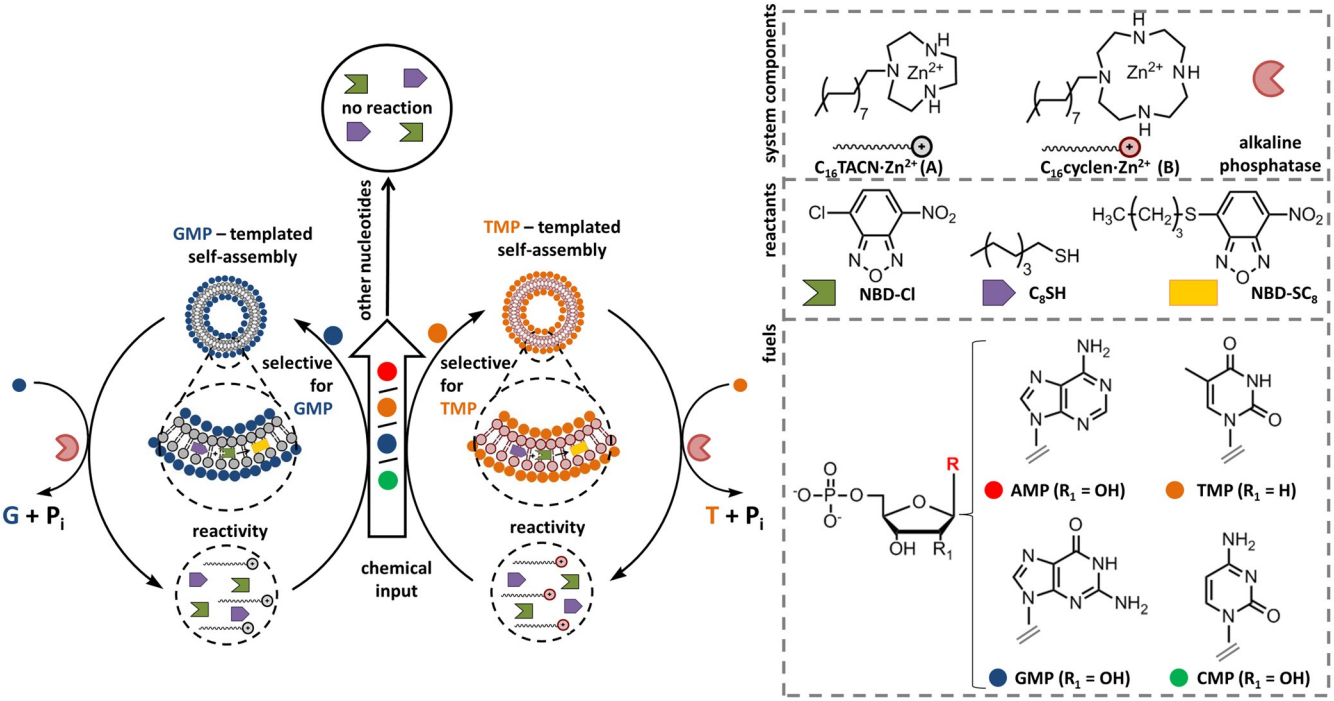

Figure 1. Schematic representation of nucleotide-selective templated self-assembly of nanoreactors under dissipative conditions and consequent transient activation of a chemical reaction between C_8-SH and NBD-Cl.

formation is a general strategy for controlling self-assembly processes, it lacks one hallmark of biological systems, which is selectivity.[29,30,42,43] Selectivity implies that only specific molecules can induce an effect and is therefore a key element to control self-assembly in complex mixtures. It is hard to achieve this using just electrostatic interactions even though we have shown in the past that TACN·Zn^{2+} has a higher affinity for phosphates compared to carboxylates.[44] Our strategy to introduce selectivity in templated self-assembly is based on recent results by our group which revealed that the affinity of monophosphate nucleosides for monolayer protected gold nanoparticles depended on the type of macrocyclic Zn^{2+}-complex present in the monolayer.[45] Thus, nanoparticles covered with a 1,4,7-triazacyclononane (TACN)·Zn^{2+} complex had a higher affinity for GMP (over TMP, CMP, and AMP), whereas the presence of 1,4,7,10-tetraazacyclododecane (cyclen)·Zn^{2+} evoked selectivity for TMP. These differences were ascribed to noncovalent interactions between the nucleobase and the macrocycle·Zn^{2+}-complexes.[46] Based on these observations, we hypothesized that the selective interaction between monophosphate nucleosides and TACN- or cyclen-functionalized amphiphiles would be a viable way to introduce selectivity in the templated self-assembly of amphiphile-based structures.[47]

In addition to the previously reported amphiphile C_{16}TACN·Zn^{2+} (**A**) containing the 1,4,7-triazacyclonane (TACN)-macrocycle, we synthesized a new amphiphile C_{16}cyclen·Zn^{2+} (**B**) containing the 1,4,7,10-tetraazacyclododecane (cyclen)-macrocycle (Figure 1). Fluorescence titrations revealed a CAC of around 100 μM for **B** in aqueous buffer at pH 7.0, which is similar to the CAC of **A** under the same conditions (Figure S4). The propensity of mono-, di-, and triphosphate nucleosides (*N*TP, *N*DP, and *N*MP, respectively, with *N* = A, T, C or G) to stabilize assemblies of **A** and **B** was measured by titrating increasing amounts of each nucleotide to a 30 μM solution of the amphiphile in aqueous buffer at pH 7.0 (Figure 2a for *N*MP and Figure S5 and S6 for *N*TP and *N*DP, respectively). This concentration is below the CAC of both **A** and **B**, which implies that no well-defined assemblies are present in the absence of nucleotides. The fluorescent apolar probe 1,6-diphenyl-1,3,5-hexatriene (DPH, 2.5 μM, $\lambda_{ex} = 355$ nm, $\lambda_{em} = 428$ nm) was added as a reporter for assembly formation.[39] DPH is highly soluble in the hydrophobic part of the assemblies and consequently a significant increase in fluorescence intensity is observed when assemblies are formed. The titration experiments showed that all nucleotides templated assembly formation, which confirmed that the strategy of counter-ion induced templation, is a general one.[48,49] Yet, significant differences were observed between *N*TP and *N*DP on one hand and *N*MP on the other hand. For all di- and triphosphate nucleosides, assembly occurred under saturation conditions for both **A** and **B** and was complete at around 15 μM of nucleotide (Figure S5, S6). This indicated that the affinity originating from the electrostatic interaction between nucleotide and amphiphile is high enough to ensure quantitative complex formation at these concentrations. This has the important consequence that selectivity as a result of other potential interactions cannot be observed for di- and triphosphate nucleosides. On the other hand, for the monophosphate nucleosides—with a lower charge—a different behaviour was observed (Figure 2a). Assembly formation required in general higher nucleotide concentrations (10–100 μM) but was strongly dependent on the nucleobase. In the case of **A**, GMP induced an increase in

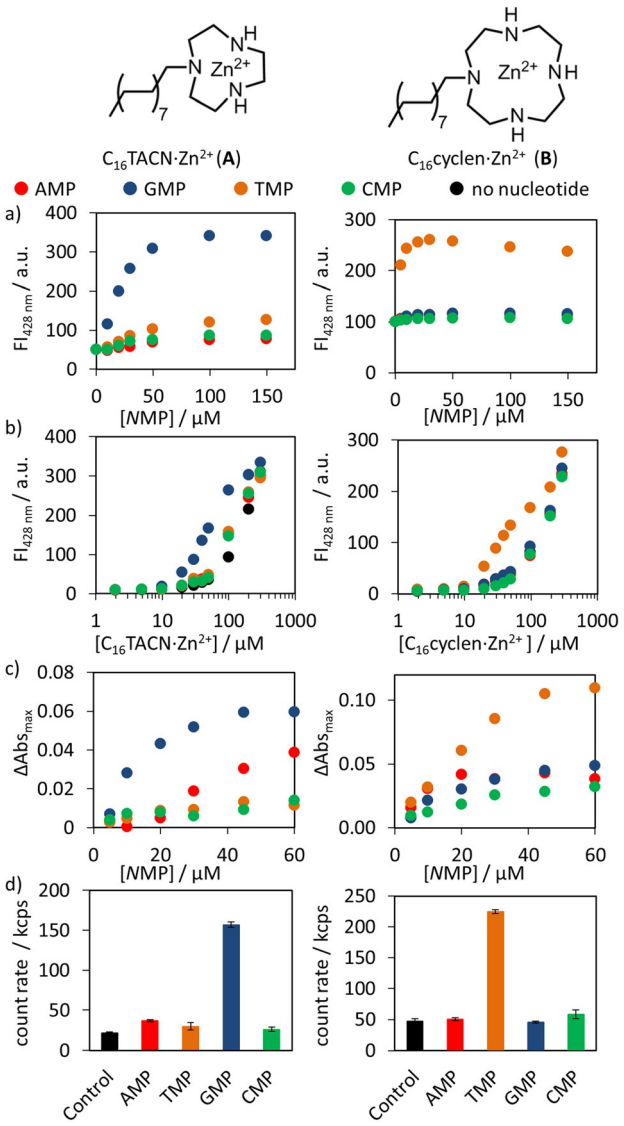

Figure 2. Fluorescence intensity at 428 nm (a) as a function of the *N*MP concentration (*N* = G, T, A, or C) at a fixed amphiphile concentration of 30 μM **A** (left graph) or **B** (right graph) in the presence of DPH (2.5 μM) and (b) as a function of the amount of amphiphile added (left graph: **C_{16}TACN·Zn^{2+} (A)**, right graph: **C_{16}cyclen·Zn^{2+} (B)**) to an aqueous buffer solution in the presence of a fixed concentration of *N*MP (30 μM). Excitation wavelength = 355 nm, slit width (ex/em) = 5/10 nm. c) Difference in absorbance at the respective absorbance maxima (AMP = 259 nm, TMP = 268 nm, GMP = 253 nm, CMP = 272 nm) of the nucleotides in the presence and absence of amphiphile as a function of the nucleotide concentration (0–60 μM) added to a solution of amphiphile (30 μM) (left graph: **C_{16}TACN·Zn^{2+} (A)**, right graph: **C_{16}cyclen·Zn^{2+} (B)**). d) Scattering intensity rate (count rate, kcps) measured by dynamic light scattering (DLS) of the aggregates formed in the absence and presence of *N*MPs (30 μM) and a fixed amount of surfactant (30 μM) (left graph: **C_{16}TACN·Zn^{2+} (A)**, right graph: **C_{16}cyclen·Zn^{2+} (B)**). All measurements were performed in triplicate. Experimental conditions: [HEPES] = 5 mM, pH 7.0, T = 25 °C.

fluorescence at lower concentrations (0–30 μM) before saturating at around 50 μM occurred. For the other nucleotides, higher concentrations were needed to observe an increase in fluorescence intensity, indicative of a weaker templating effect. A differential response to the nucleotides was also observed for **B**, except that in this case it was TMP that induced an increase in fluorescence intensity at low micromolar concentrations (0–20 μM). The selectivity of GMP for **A** and TMP for **B** emerged likewise from fluorescence titrations in which the concentration of the amphiphiles (**A** and **B**) was gradually increased in the presence of a constant concentration of *N*MP (30 μM; N = A, T, G or C) and DPH (2.5 μM)(Figure 2b). GMP caused the strongest decrease in the CAC (≈20 μM) in the case of **A** and TMP caused the strongest decrease in the CAC (≈20 μM) of **B**.

The ability of GMP and TMP to trigger assembly formation of **A** and **B**, respectively, at lower concentrations compared to other monophosphate nucleosides was confirmed by other techniques. UV-vis spectra were measured for all monophosphate nucleosides in the 0–60 μM concentration regimes in the absence and presence of the surfactant (Figure 2c). When the difference in absorbance at the respective absorbance maxima (AMP = 259 nm, TMP = 268 nm, GMP = 253 nm, CMP = 272 nm) of the nucleotides in the presence and absence of amphiphile (**A** and **B**) was plotted as a function of the nucleotide concentration, a maximum difference in absorbance of GMP was observed in the case of **A** and of TMP in the case of **B**. Apart from confirming the selectivity, these observations also indicate a direct interaction between the nucleobase and the Zn^{2+}-macrocycle (TACN in **A**, cyclen in **B**). Indeed, it is well-documented that Zn^{2+}-macrocycle complexes selectively interact with nucleobases as a result of coordination bonds between donor atoms of the nucleobase and the Zn^{2+}-metal ion in combination with hydrogen bonds that involve the NH-moieties present in the macrocycle.[49–51]

The dynamic light scattering (DLS) intensity (count rate, kcps) increased significantly only when GMP (30 μM) was added to a solution of **A** (30 μM) or TMP (30 μM) to a solution of **B** (30 μM), but not for either one of the other combinations (Figure 2d). Finally, laser scanning confocal microscopy studies (LSCM) permitted a direct visualization of assembly formation. Although the size of these assemblies is lower than the resolution of this optical technique, the accumulation of the hydrophobic probe Coumarin 153 (C153) in the apolar part of the assemblies resulted in an increase in local concentration which was detectable. The formation of assemblies was observed only upon the addition of GMP to **A** or TMP to **B** (Figure 3a,b).

Next, we analysed the structure of the selective *N*MP-templated assemblies **A**·GMP and **B**·TMP by DLS and transmission electron microscopy (TEM) (Figure 4). We performed a series of DLS measurements of solutions containing a constant concentration of surfactants, **A** and **B** (30 μM) and varying concentrations of either GMP or TMP (10–150 μM), respectively. Stable assemblies with a well-defined size were obtained for GMP concentrations between 30 and 120 μM in the case of **A** and TMP concentrations between 20 and 80 μM in the case of **B** (Figure 4b and Figure S9). At lower concentrations, no reproducible size could be measured, whereas at higher concentrations large aggregates were observed and, eventually, precipitated. In the stable range, an average assembly size of 45 ± 10 nm for

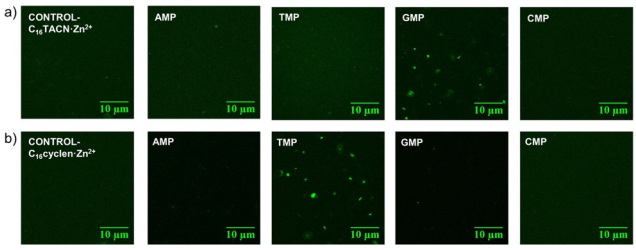

Figure 3. Fluorescence confocal images taken 20 min after mixing a) **A** or b) **B** and either one of the nucleotides. Experimental conditions: Amphiphile (30 μM), coumarin C153 (2.5 μM) and *N*MP (30 μM). Experimental conditions: [HEPES] = 5 mM, pH 7.0, T = 25 °C.

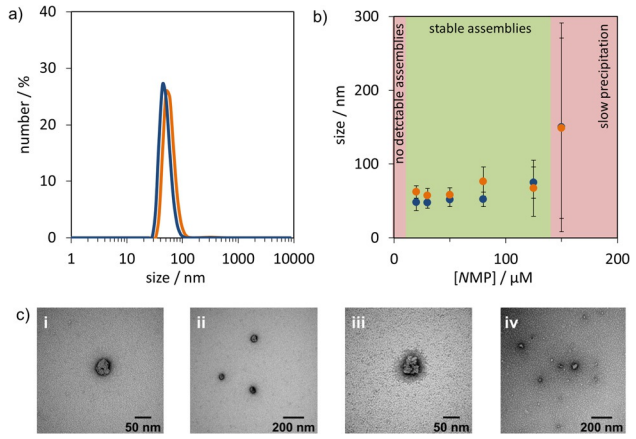

Figure 4. a) Representative DLS graphs of solutions containing **A** and **GMP** (30 μM each, blue trace) or **B** and **TMP** (30 μM each, orange trace). Experimental conditions: [HEPES] = 5 mM, pH 7, T = 25 °C. b) Hydrodynamic diameters measured with DLS as a function of NMP concentration (10–150 μM) at a constant amphiphile concentration (30 μM) in HEPES buffer (pH 7, 5 mM). Blue dots correspond to the **A**·GMP system and orange dots correspond to **B**·TMP system. The green area indicates the concentration regime at which stable assemblies were observed. c) TEM images of a solution containing NMP (30 μM) and amphiphile (30 μM) in HEPES buffer (pH 7, 5 mM). i–ii) TEM images of **A**·GMP, iii–iv) TEM images of **B**·TMP. Samples were stained with 2% uranyl acetate solution.

A·GMP and 55 ± 10 nm for **B**·TMP was determined (Figure 4a). TEM images revealed the formation of spherical structures with similar dimensions (Figure 4c and Figure S11–S13). Altogether, these data show that monophosphate nucleosides selectively template the formation of nanosized-assemblies, which, according to the UV-vis studies, is ascribed to additional stabilizing interactions originating from interactions between guanine and the TACN·Zn^{2+}-complex in **A** and thymidine and the cyclen·Zn^{2+}-complex in **B**.

Next, we shifted our attention towards studying *N*MP-templated assembly formation under dissipative conditions installed by the dephosphorylating enzyme alkaline phosphatase (AP)[49] (Figure 5). Only upon the addition of GMP to a solution containing **A** (30 μM), DPH (2.5 μM) and AP (1 U mL^{-1}) or upon the addition of TMP to a similar solution containing **B** instead of **A**, a transient increase in fluorescence intensity was observed indicating transient self-assembly

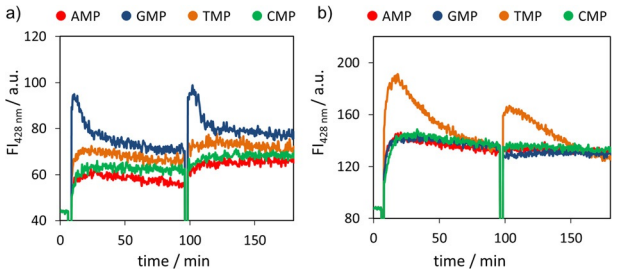

Figure 5. Fluorescence intensity at 428 nm following two repetitive additions of NMP (30 μM; N = A, T, G, C) to a solution of a) **A** (30 μM) or b) **B** (30 μM) and DPH (2.5 μM) in the presence of alkaline phosphatase (AP) (1 U mL^{-1}). Experimental conditions: [HEPES] = 5 mM, pH 7, T = 25 °C.

(Figure 5a,b). All other combinations of nucleotides and amphiphiles failed to show a similar effect. It was observed that the half-life of transient assemblies **A**·GMP, measured as the time to reduce the fluorescence intensity from the maximum to end value, was 30 minutes compared to 60 minutes for the combination **B**·TMP, attributed to the lower rates at which the nucleotides are hydrolysed. The cycles could be re-initiated by adding new batches of the respective nucleotide, which showed the reversible nature of this process. The lower efficiency of successive cycles in the respective systems (**A**·GMP and **B**·TMP) most probably originated from the accumulation of waste product. Further evidence for transient assembly formation in the presence of AP was obtained from DLS. Addition of GMP to a solution of **A** and AP resulted in the rapid formation of structures with a hydrodynamic diameter of 45 ± 10 nm, which in around 30 minutes decreased to a size of 17 ± 10 nm. This end value corresponded to that observed for **A** in the presence of the waste products of GMP hydrolysis (guanosine + P_i). A similar behaviour was observed when TMP was added to a solution of **B** and AP. In this case, the hydrodynamic diameter decreased from 55 ± 10 nm to 21 ± 5 nm in around 60 minutes. Also, this end value corresponded to the one observed when the waste products of TMP hydrolysis (thymidine + P_i) were added to **B** (Figure S16).

The selective formation of assemblies implies that any chemical function associated exclusively to the assembled state can be selectively activated. Because of our interest in developing network reactivity, we have a special interest in exploiting the ability of the templated assemblies to accelerate chemical reactions. Previously, we have shown that ATP-templated vesicles acted as nanoreactors by strongly accelerating, compared to the background reaction in aqueous buffer, a nucleophilic aromatic substitution reaction between two hydrophobic molecules, 4-chloro-7-nitrobenzofurazan (NBD-Cl) and octane thiol (C_8-SH).[39] The driving force for rate acceleration was the uptake of both reactants in the apolar bilayer which led to an increase in local concentration. Here, as an important step towards the selective activation of reaction pathways in complex mixtures we investigated whether we could exploit nucleotide-selective templation to trigger chemical reactivity with selective inputs. The reaction between NBD-Cl (1.5 μM) and C_8-SH (2.0 μM)

was studied in solutions of **A** or **B** (30 μM) to which either one of the monophosphate nucleosides (*N*MP; N = A, T, G or C, 30 μM) was added. An excess of $Zn(NO_3)_2$ (600 μM) was added to suppress a slow side reaction between NBD-Cl and the head groups. The reaction progress was monitored both by UPLC and UV-vis spectroscopy, following the increase in absorbance at 420 nm originating from the product formed by the two hydrophobic reactants (NBD-SC_8) (Figure 6a,d). Importantly, in the presence of amphiphile **A** only the addition of GMP resulted in a strong increase in rate (> 10-fold based on the first 15 minutes) compared to the reference system to which no nucleotide was added (Figure 6b). The addition of any of the other nucleotides caused just a very small increase in rate compared to the background. A difference in rate between GMP and the other nucleotides was not observed in the absence of the surfactant C_{16}TACN·Zn^{2+}, which indicates that amphiphile **A** plays an essential role in inducing rate acceleration (Figure S24). Finally, the correlation between GMP and reactivity was confirmed by measuring the rate as a function of GMP concentration. A clear increase in the initial rate was observed up to around 20 μM of GMP after which the rate remained constant (Figure 6c). This is an important observation as it underlines the working principle of the system: the maximum effect of GMP on rate acceleration is determined by the amount of assemblies that can be templated by a given concentration of GMP. Importantly, the selectivity completely changed when amphiphile **B** was used instead of **A**. For this amphiphile, an increase in rate was only observed when TMP was added and not for any of the other nucleotides (Figure 6b). Similar to the **A**·GMP system, a clear increase in rate was observed for concentrations up to 20 μM of nucleotide after which the rate remained constant (Figure 6c). The observed differential responses of the **A** and **B** systems to nucleotides clearly establish a connection between selectivity in templated-assembly and reaction pathway activation.

A key characteristic of biological systems is that reaction pathways are transiently up- or downregulated caused by the temporary availability of a trigger.[52,53] We therefore studied nucleotide-selective transient reaction activation under dissipative conditions by following formation of product NBD-SC_8. UPLC studies revealed that in the absence of the enzyme AP the product concentration increased gradually in time to reach a maximum value after around 70 minutes for both systems (**A**·GMP and **B**·TMP) (Figure 7a). However, in the presence of enzyme (3 U mL^{-1} for **A**·GMP and 6 U mL^{-1} for **B**·TMP) the product concentration ceased to increase much earlier after addition of GMP or TMP, respectively, and reached a lower final concentration (Figure 7a). This shows that product formation is governed by the assembly lifetime. Importantly, the addition of a second batch of GMP to the **A**-system caused an additional transient burst in product formation. On the other hand, the addition of TMP did not lead to any increase evidencing the selective nature of transient pathway activation (Figure 7b). Transient up-regulation was also observed for the **B**-system, but in this case only when TMP was added instead of GMP (Figure 7b).

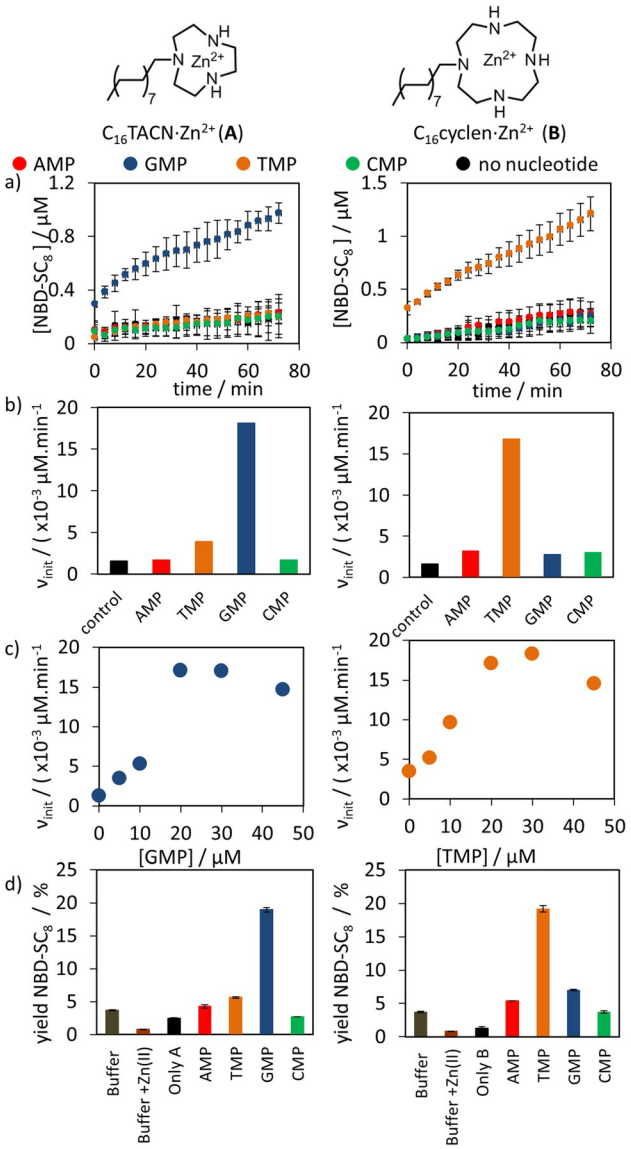

Figure 6. a) Concentration of the product NBD-SC_8 as a function of time measured by UV-vis upon the addition of either one of the nucleotides NMP (30 μM) to a solution of amphiphile (30 μM; left graph: **A**; right graph: **B**), Zn^{2+} (600 μM), NBD-Cl (1.5 μM) and C_8-SH (2 μM) in HEPES buffer (pH 7, 5 mM) at 25 °C. The background reaction (without nucleotides) is marked with the black indicators. All measurements were performed in triplicate. b) Initial reaction rates (0–10 minutes) as a function of the kind of nucleotide *N*MP (30 μM) added to either **A** (left graph) or **B** (right graph). The initial rate of the background reaction is marked with the black indicators. (c) Initial reaction rates (0–10 minutes) as a function of the concentration of **GMP** (0–45 μM; left graph) or **TMP** (0–45 μM; right graph) added to a solution of **A** or **B**, respectively. d) Yield (%) of the product NBD-SC_8, 20 minutes after the addition of NMP (30 μM) to a solution containing either **A** (30 μM, left graph) or **B** (30 μM, right graph) and Zn^{2+} (600 μM), NBD-Cl (1.5 μM) and C_8-SH (2 μM) in HEPES buffer (pH 7, 5 mM) at 25 °C. The blanks include: only buffer, buffer + Zn^{2+} (600 μM) and only amphiphile **A** (left graph) or **B** (right graph).

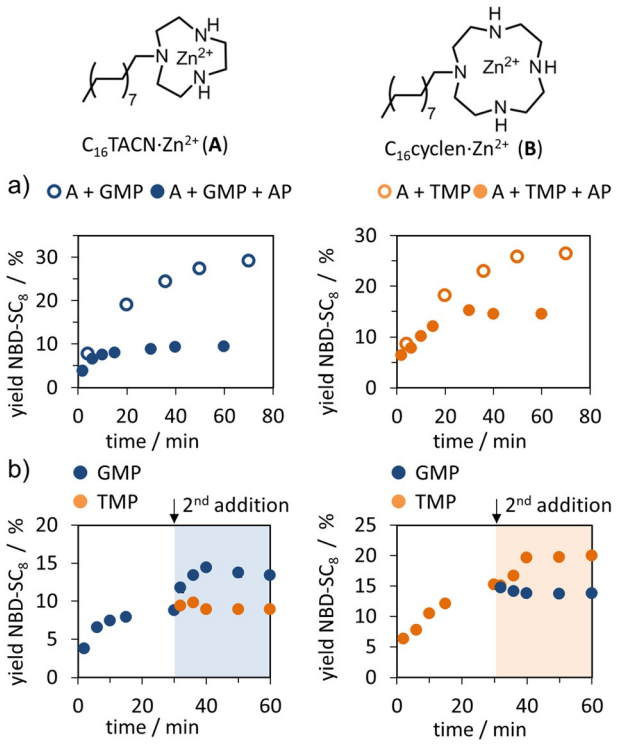

Figure 7. Yield (%) of the product NBD-SC_8 as a function of time in a solution containing a) **A** (30 μM, left graph) or **B** (30 μM, right graph), Zn^{2+} (600 μM), NBD-Cl (1.5 μM), C_8-SH (2 μM), **GMP** (30 μM, left graph) or **TMP** (30 μM, right graph), with AP (solid dots; 3 U mL^{-1}, top graph; 6 U mL^{-1}, bottom graph) and without AP (hollow dots). b) Amphiphile (30 μM; left graph: **A**; right graph: **B**), Zn^{2+} (600 μM), NBD-Cl (1.5 μM), C_8-SH (2 μM), AP (3 U mL^{-1}, left graph; 6 U mL^{-1}, right graph). Blue dots represent **GMP** and orange dots represent **TMP**. The coloured regions in (b) represent the second addition of NMP after 30 minutes. Experimental conditions: HEPES buffer (pH 7, 5 mM) at 25 °C.

Conclusion

In conclusion, we have shown that the self-assembly of nanoreactors can be selectively triggered by adding monophosphate nucleosides to the mixture. The selectivity originates from the selective non-covalent interactions between the head groups of the amphiphile and the nucleotide. Under dissipative conditions, installed by the presence of the enzyme alkaline phosphatase, the assemblies have a limited lifetime. The transient assemblies act as nanoreactors for a bimolecular reaction between two apolar reagents. Under dissipative conditions the up-regulation of chemical reactivity becomes a transient phenomenon, while preserving selectivity. Templated self-assembly under dissipative conditions offers an attractive way to control the functional properties of a complex mixture. This enables new possibilities for developing synthetic chemical reaction networks that can control the behaviour of next-generation materials.

Acknowledgements

This work was financially supported by the European Commission (grant MSCA 657486), the Italian Ministry of Education and Research (grant 2017E44A9P) and the University of Padova (CPDA155454).

Conflict of interest

The authors declare no conflict of interest.

Keywords: amphiphiles · molecular recognition · network reactivity · self-assembly · systems chemistry

[1] J. J. Tyson, K. C. Chen, B. Novak, *Curr. Opin. Cell Biol.* **2003**, *15*, 221–231.
[2] O. R. Maguire, W. T. S. Huck, *Emerg. Top. Life. Sci.* **2019**, *3*, 517–527.
[3] M. P. McNerney, M. P. Styczynski, *Wiley Interdiscip. Rev. Syst. Biol. Med.* **2018**, *10*, e1405.
[4] G. M. Whitesides, R. F. Ismagilov, *Science* **1999**, *284*, 89–92.
[5] C. J. Gerdts, D. E. Sharoyan, R. F. Ismagilov, *J. Am. Chem. Soc.* **2004**, *126*, 6327–6331.
[6] H. W. H. van Roekel, B. Rosier, L. H. H. Meijer, P. A. J. Hilbers, A. J. Markvoort, W. T. S. Huck, T. F. A. de Greef, *Chem. Soc. Rev.* **2015**, *44*, 7465–7483.
[7] G. Ashkenasy, T. M. Hermans, S. Otto, A. F. Taylor, *Chem. Soc. Rev.* **2017**, *46*, 2543–2554.
[8] G. Lebon, D. Jou, J. Casas-Vázquez, *Understanding Non-equilibrium Thermodynamics: Foundations, Applications, Frontiers*, Springer Berlin Heidelberg, Berlin, **2008**.
[9] S. C. Warren, O. Guney-Altay, B. A. Grzybowski, *J. Phys. Chem. Lett.* **2012**, *3*, 2103–2111.
[10] B. A. Grzybowski, W. T. S. Huck, *Nat. Nanotechnol.* **2016**, *11*, 584–591.
[11] S. J. Jones, A. F. Taylor, P. A. Beales, *Exp. Biol. Med.* **2019**, *244*, 283–293.
[12] K. Montagne, R. Plasson, Y. Sakai, T. Fujii, Y. Rondelez, *Mol. Syst. Biol.* **2011**, *7*, 466.
[13] G. Ashkenasy, R. Jagasia, M. Yadav, M. R. Ghadiri, *Proc. Natl. Acad. Sci. USA* **2004**, *101*, 10872–10877.
[14] S. N. Semenov, A. S. Y. Wong, R. M. van der Made, S. G. J. Postma, J. Groen, H. W. H. van Roekel, T. F. A. de Greef, W. T. S. Huck, *Nat. Chem.* **2015**, *7*, 160–165.
[15] S. N. Semenov, L. J. Kraft, A. Ainla, M. Zhao, M. Baghbanzadeh, V. E. Campbell, K. Kang, J. M. Fox, G. M. Whitesides, *Nature* **2016**, *537*, 656–660.
[16] I. Lagzi, D. W. Wang, B. Kowalczyk, B. A. Grzybowski, *Langmuir* **2010**, *26*, 13770–13772.
[17] I. Lagzi, B. Kowalczyk, D. W. Wang, B. A. Grzybowski, *Angew. Chem. Int. Ed.* **2010**, *49*, 8616–8619; *Angew. Chem.* **2010**, *122*, 8798–8801.
[18] J. W. Szostak, *Philos. Trans. R. Soc. London Ser. B* **2011**, *366*, 2894–2901.
[19] S. Otto, *Acc. Chem. Res.* **2012**, *45*, 2200–2210.
[20] H. Zhao, S. Sen, T. Udayabhaskararao, M. Sawczyk, K. Kucanda, D. Manna, P. K. Kundu, J. W. Lee, P. Kral, R. Klajn, *Nat. Nanotechnol.* **2016**, *11*, 82–88.
[21] A. Pross, *Emerg. Top. Life. Sci.* **2019**, *3*, 435–443.
[22] A. B. Grommet, M. Feller, R. Klajn, *Nat. Nanotechnol.* **2020**, *15*, 256–271.

[23] J. Boekhoven, A. M. Brizard, K. N. K. Kowlgi, G. J. M. Koper, R. Eelkema, J. H. van Esch, *Angew. Chem. Int. Ed.* **2010**, *49*, 4825 – 4828; *Angew. Chem.* **2010**, *122*, 4935 – 4938.
[24] J. Boekhoven, W. E. Hendriksen, G. J. M. Koper, R. Eelkema, J. H. van Esch, *Science* **2015**, *349*, 1075 – 1079.
[25] S. Debnath, S. Roy, R. V. Ulijn, *J. Am. Chem. Soc.* **2013**, *135*, 16789 – 16792.
[26] C. Pezzato, L. J. Prins, *Nat. Commun.* **2015**, *6*, 7790.
[27] T. Heuser, E. Weyandt, A. Walther, *Angew. Chem. Int. Ed.* **2015**, *54*, 13258 – 13262; *Angew. Chem.* **2015**, *127*, 13456 – 13460.
[28] S. Dhiman, A. Jain, M. Kumar, S. J. George, *J. Am. Chem. Soc.* **2017**, *139*, 16568 – 16575.
[29] A. Jain, S. Dhiman, A. Dhayani, P. K. Vemula, S. J. George, *Nat. Commun.* **2019**, *10*, 450.
[30] A. Sorrenti, J. Leira-Iglesias, A. Sato, T. M. Hermans, *Nat. Commun.* **2017**, *8*, 15899.
[31] M. Tena-Solsona, B. Riess, R. K. Grotsch, F. C. Lohrer, C. Wanzke, B. Kasdorf, A. R. Bausch, P. Muller-Buschbaum, O. Lieleg, J. Boekhoven, *Nat. Commun.* **2017**, *8*, 15895.
[32] M. Tena-Solsona, C. Wanzke, B. Riess, A. R. Bausch, J. Boekhoven, *Nat. Commun.* **2018**, *9*, 2044.
[33] S. M. Morrow, I. Colomer, S. P. A. Fletcher, *Nat. Commun.* **2019**, *10*, 1011.
[34] H. L. Che, S. P. Cao, J. C. M. van Hest, *J. Am. Chem. Soc.* **2018**, *140*, 5356 – 5359.
[35] P. Solís Muñana, G. Ragazzon, J. Dupont, C. Z. J. Ren, L. J. Prins, J. L.-Y. Chen, *Angew. Chem. Int. Ed.* **2018**, *57*, 16469 – 16474; *Angew. Chem.* **2018**, *130*, 16707 – 16712.
[36] Z. Li, C. J. Zeman, S. R. Valandro, J. P. O. Bantang, K. S. Schanze, *J. Am. Chem. Soc.* **2019**, *141*, 12610 – 12618.
[37] S. Bal, K. Das, S. Ahmed, D. Das, *Angew. Chem. Int. Ed.* **2019**, *58*, 244 – 247; *Angew. Chem.* **2019**, *131*, 250 – 253.
[38] C. Wanzke, A. Jussupow, F. Kohler, H. Dietz, V. R. I. Kaila, J. Boekhoven, *ChemSystemsChem* **2020**, *2*, e1900044.
[39] S. Maiti, I. Fortunati, C. Ferrante, P. Scrimin, L. J. Prins, *Nat. Chem.* **2016**, *8*, 725 – 731.
[40] M. A. Cardona, L. J. Prins, *Chem. Sci.* **2020**, *11*, 1518 – 1522.
[41] J. L.-Y. Chen, S. Maiti, I. Fortunati, C. Ferrante, L. J. Prins, *Chem. Eur. J.* **2017**, *23*, 11549 – 11559.
[42] H. Ischiropoulos, *Biochem. Biophys. Res. Commun.* **2003**, *305*, 776 – 783.
[43] M. Wright, J. M. Diamond, *Physiol. Rev.* **1977**, *57*, 109 – 156.
[44] C. Pezzato, P. Scrimin, L. J. Prins, *Angew. Chem. Int. Ed.* **2014**, *53*, 2104 – 2109; *Angew. Chem.* **2014**, *126*, 2136 – 2141.
[45] F. della Sala, S. Maiti, A. Bonanni, P. Scrimin, L. J. Prins, *Angew. Chem. Int. Ed.* **2018**, *57*, 1611 – 1615; *Angew. Chem.* **2018**, *130*, 1627 – 1631.
[46] S. Aoki, E. Kimura, *J. Am. Chem. Soc.* **2000**, *122*, 4542 – 4548.
[47] A. Mishra, D. B. Korlepara, M. Kumar, A. Jain, N. Jonnalagadda, K. K. Bejagam, S. Balasubramanian, S. J. George, *Nat. Commun.* **2018**, *9*, 1295.
[48] N. Vlachy, M. Drechsler, J. M. Verbavatz, D. Touraud, W. Kunz, *J. Colloid Interface Sci.* **2008**, *319*, 542 – 548.
[49] Z. W. Guo, N. Hauser, A. Moreno, T. Ishikawa, P. Walde, *Soft Matter* **2011**, *7*, 180 – 193.
[50] R. B. Martin, *Acc. Chem. Res.* **1985**, *18*, 32 – 38.
[51] S. Aoki, E. Kimura, *Chem. Rev.* **2004**, *104*, 769 – 787.
[52] R. Maithreye, R. R. Sarkar, V. K. Parnaik, S. Sinha, *Plos One* **2008**, *3*, e2972.
[53] M. Dzialo, J. Szopa, T. Czuj, M. Zuk, *Front. Plant Sci.* **2017**, *8*, 755.

Manuscript received: July 25, 2020
Accepted manuscript online: August 24, 2020
Version of record online: September 29, 2020

